havior of this system is analogous to that for C_nMV^{2+}–DHP reduction by SO_2^- ion.[8] In the latter system, circumstantial evidence was obtained suggesting that transmembrane redox is carried only by electron exchange between the "buried" viologens.[28] Exposition of the molecular organization at the reactive sites is therefore crucial to developing an understanding of transmembrane redox processes.[6] To this end, we are currently studying viologen-DHP interactions by a variety of structural techniques.

Acknowledgment. Financial support for this research was provided by a grant from the Division of Chemical Sciences, U.S. Department of Energy (Grant No. DE-AC-06-83ER13111). The digital oscilloscope used in the fast-kinetics studies was obtained through a grant (Grant No. 8522) from the Medical Research Foundation of Oregon. The authors are deeply grateful to these agencies for their program support. It is also a pleasure to acknowledge stimulating discussions with Dr. James Espenson concerning reaction mechanisms, the assistance of Eberhardt Kuhn in analyzing some of the data, and the interest of Dr. William C. Barrette, Jr., who first suggested this study.

---

[28] Attempts to study transmembrane redox in this system were obviated because the C_nMV^{2+} ions underwent extensive degradation under the conditions required for DHP vesicle formation, i.e., high temperature and alkaline media. It was not possible, therefore, to prepare vesicles with C_nMV^{2+} bound at both interfaces.

Contribution from the Department of Chemistry, Willard Hall,
Kansas State University, Manhattan, Kansas 66506

Cleavage Reactions of Bridged Structures. Asymmetric Cleavage of Diborane: A Case of Counterintuitive Orbital Control of Reaction Products

Keith F. Purcell* and David D. Devore

Received April 23, 1986

As prototypes of inorganic bridge structure cleavage reactions by Lewis base attack, those of diborane are of two types: symmetric (2 LBH_3 as product) and asymmetric ($L_2BH_2^+BH_4^-$ as product). The known structure ($(LBH_2)H(BH_3)$) likely appears as an intermediate in these cleavage reactions and serves as a model for the microstudy of the cleavage. This article addresses the question of orbital steering of the second ligand-interchange step of L for H(bridge) at boron, the step that consummates the cleavage reactions. We conclude that there is electronic steering favoring geminal (asymmetric) entry of the second Lewis base molecule. Generalization of our findings for this molecule clarifies the roles of the electronegativity and orbital type of the bridge atom and of the long-range bridgefoot orbital interference energies in the general phenomenon of cleavage of inorganic bridge structures, of which $(LBH_2)H(BH_3)$ is but one example.

Introduction

Inorganic bridged structures are pervasive, and bridge-cleavage reactions are of fundamental importance to electron-transfer, mixed-valence and polynuclear catalysis reactions. While there have been many investigations of bridge electronic structures, much less attention has been given to understanding how such bridges are cleaved by Lewis acids and bases. The works of Shore, of Parry, and of Jolly on the cleavage of diborane by Lewis bases present an interesting case, with cleavage leading to either of two types of products: simple borane adducts result from symmetric cleavage (eq 1), and salts are produced from unsymmetric cleavage (eq 2).[1] It is to be presumed that these cleavage reactions proceed

$$B_2H_6 + 2L \rightarrow 2LBH_3 \qquad (1)$$

$$B_2H_6 + 2L \rightarrow L_2BH_2^+BH_4^- \qquad (2)$$

through a common "half-opened" intermediate, LB_2H_6, resulting from an interchange attack by a single L molecule upon B_2H_6. In fact, the "half-opened" structures have been prepared independently through reactions like (3).[2] The cleavage of **1** is geminal

$$2LBH_3 + B_2H_6 \rightarrow \underset{\mathbf{1}}{2(LBH_2)H(BH_3)} \qquad (3)$$

(B_g) or vicinal (B_v) to the substituted boron and may proceed by a B–H_b dissociative reaction step or by a ligand-interchange step of L for H_b.

The experimental product distributions observed for sterically hindered and unhindered donors suggest that, in the absence of steric factors, asymmetric cleavage is favored (reaction 2). To account for this observation, one can propose either dissociative cleavage of **1** at B_g–H_b or ligand interchange at B_g involving L–B_g bond-forming and B_g–H_b bond-breaking components. At first glance, the experimental result might be attributed simply to an interchange step with classical electrostatic forces directing L to the more electrophilic boron atom, B_g. The same forces operating within **1** would, however, favor stronger B_g–H_b than H_b–B_v bonding, favoring reaction 1 in either a dissociative or interchange step. Even more troublesome to us is the naiveté of such classical arguments in ignoring the orbital interference requirements of interchange and dissociative reaction steps. To complicate matters, the steric congestion differential for B_g and B_v should direct L to B_v, generally.

These questions merit an analysis of the *electronic* control by intermediate **1** of the site of entry of L in the second interchange step.[4,5] The primary conclusion of this report is that there is electronic steering of the second donor to B_g in **1**, whether the cleavage is dissociative or associative, and that this geminal regiospecificity is soundly based in the orbital topology of the three-center bridge unit. Furthermore, we have been able to establish the requirements for chemical tuning of this topology to select geminal or vicinal attack.

Calculational Methods

Standard INDO calculations[6] were performed for the "half-opened" intermediate $(H_3NBH_2)H(BH_3)$ using tetrahedral angles and representative bond distances; Figure 1 presents a representation of the structure of the "half-open" intermediate in the presence of an approaching NH_3 molecule.

The INDO molecular orbital functions were renormalized with overlap integrals included in order to obtain more realistic contour maps of orbital amplitudes.[7] The graphical presentations given here result from calcu-

---

[1] McAchran, G. E.; Shore, S. G. *Inorg. Chem.* **1965**, *4*, 125. Shore, S. G.; Hickam, C. W.; Cowles, D. *J. Am. Chem. Soc.* **1965**, *87*, 2755. Rudolph, R. W.; Parry, R. W.; Farran, C. F. *Inorg. Chem.* **1966**, *5*, 723. Schultz, D. R.; Parry, R. W. *J. Am. Chem. Soc.* **1958**, *80*, 4. Shore, S. G. *Ibid.* **1958**, *80*, 8. Beachley, O. T. *Inorg. Chem.* **1965**, *4*, 1823. Finn, P.; Jolly, W. L. *Ibid.* **1972**, *11*, 1941.

[2] Shore, S. G.; Hall, C. L. *J. Am. Chem. Soc.* **1966**, *88*, 5346. Shore, S. G.; Hall, C. L. *Ibid.* **1967**, *89*, 3947.

[3] Purcell, K. F.; Kotz, J. C. *Inorganic Chemistry*; W. B. Saunders: Philadelphia, PA, 1977: (a) p 400; (b) p 109; (c) pp 657, 674.

[4] Young, D. E.; Shore, S. G. *J. Am. Chem. Soc.* **1969**, *91*, 3497.

[5] Moews, P. C., Jr.; Parry, R. W. *Inorg. Chem.* **1966**, *5*, 1552.

[6] Pople, J. A.; Beveridge, D. L. *Approximate Molecular Orbital Theory*; McGraw-Hill: New York, 1970. A locally modified version of the standard INDO program was used.

[7] Offenhartz, P. O. *Atomic and Molecular Orbital Theory*; McGraw-Hill: New York, 1970; Appendix 2.

0020-1669/87/1326-0043$01.50/0

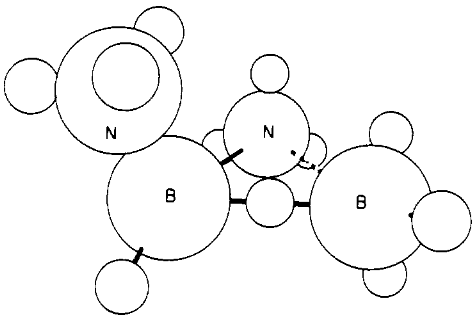

Figure 1. Molecular geometry of **1**, with a second NH_3 molecule placed behind. The *z* axis lies along the bridge axis, and N falls in the *xz* plane, which is the symmetry plane for **1**. The view is from slightly above the *yz* plane, which contains the N atom of the rear NH_3 molecule.

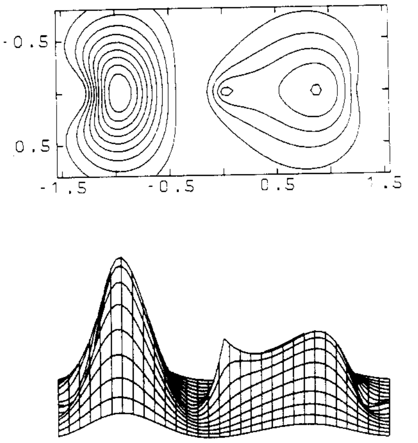

Figure 2. Contour and surface maps for the bridge LUMO density function of $H_3NB_2H_6$ (B_g appears to the left side of these diagrams).

lation of orbital amplitudes at grid points in the contour plane as input to the package SURFACE II, available from the Kansas Geological Survey[8] (the *z* axis lies along the BHB axis, with the N atom in the *xz* plane; the contour plane is the *yz* plane).

Results and Discussion

BHB Frontier Orbital Control of the Cleavage Path. Figure 2 shows the contour and perspective graphs of the bridge-region LUMO density function for the "half-open" intermediate, H_3N-B_2H_6. Two features of the LUMO are striking and decisive: the polarization toward B_g and the location of the node.

The LUMO, with greater amplitude at B_g than at B_v, steers the newly entering donor to geminal attack through LUMO overlap with the donor HOMO (lone pair). This orbital steering is reinforced by a weak electrostatic potential asymmetry, as the INDO atom charges for the three bridge atoms are found to be 0.07 (B_g), 0.04 (H), and -0.01 (B_v).

That the node for LUMO is found between B_g and the bridge hydrogen atoms facilitates the dissociation of BH_4^- from **1**; delocalization of the donor HOMO electron pair onto the substrate, in addition to commencing formation of the new B_g–L bond, weakens the B_g–H(bridge) bond while strengthening the H(bridge)–B_v bond. These LUMO characteristics nicely account for the experimental observation that geminal attack and unsymmetric cleavage of the intermediate are generally favored. After discussion of the bridge orbital topologies in the next part, it will be shown that dissociative cleavage of **1** also is asymmetric.

Effect of Lewis Basicity. Another important chemical feature of the three-center orbital topology concerns the effect of varying donor ability on orbital steering. This is of importance, for it is the engine driving the orbital polarizations and thus determines the *magnitude* of the bridge orbital polarization. In Figure 3 are presented contour maps of the bridge LUMO amplitude for the series of "half-opened" intermediates LB_2H_6, with L = H^-, NH_3, and nothing. The last member represents the limiting case of an "infinite electronegativity" donor with zero electron-donating nature. Clearly, as the donor ability of L decreases (measured in this case by the total electron density at B_g), the degree to which the LUMO is polarized toward the geminal position increases and that to the vicinal bridgefoot atom decreases; the unsymmetric bridge-cleavage path is increasingly favored the weaker the Lewis base L. As an extension, note that replacing H(terminal) in the intermediate $LBH_2(H)BH_3$ with more electronegative atoms (viz., $(LBX_2)H(BH_3)$) has an effect equivalent to that of decreasing the donor ability of the donor in $(LBH_2)H(BH_3)$; asymmetric cleavage is again favored.

Chart I

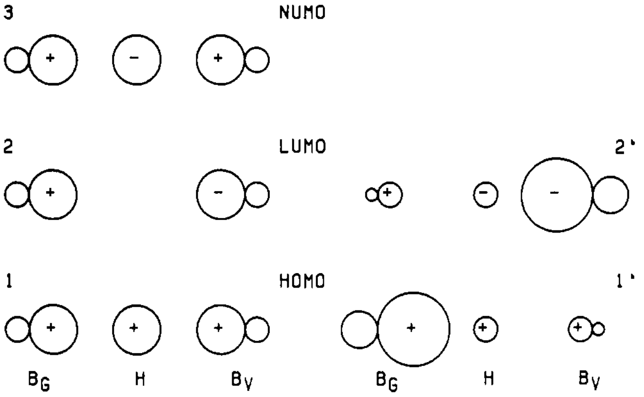

Bridge LUMO Topology. It is not apparent that the bridge LUMO should be polarized toward the substituted boron atom. Consequently, it is important to trace the origin of this polarization, not only for a complete understanding of the diborane cleavage reaction but also for the insights that result for bridge-cleavage reactions in general.

We start with $B_2H_7^-$ (=$(H_3B)H(BH_3)$) in which the LUMO node is symmetrically placed and the LUMO is not polarized. This is seen in Figure 4, where are shown the density maps for the three-center bridge orbitals. To elucidate the symmetry basis for what is to follow, note that the symmetry properties, under the inversion operation, of the NUMO, LUMO, and HOMO are S, A, and S, respectively.

Perturbation theory provides a convenient vehicle to describe the LUMO polarization when a terminal hydride of $(H_3B)H(BH_3)^-$ is replaced by L. In the customary situation of two-center orbitals, the unperturbed HOMO and LUMO are mixed with like or unlike signs, as required, to cause the HOMO to polarize in a direction to relieve the perturbational stress—an electronic Le Chatelier's principle.

When a terminal hydride ligand of $(H_3B)H(BH_3)^-$ is replaced by a less electron releasing group, the electron repulsions at the perturbed boron atom, B_g, diminish, thereby increasing the effective nuclear charge for the valence electrons of B_g. The HOMO responds by its dipolarization toward that atom, reflecting the flow of its electrons in that direction; this dipolarization is achieved by the A → S mixing of the LUMO into the HOMO. In Chart I, the LUMO is orbital 2, the HOMO is orbital 1, and the phase[9] (+ in Chart I) will increase the HOMO amplitude at the perturbed atom (1′ in Chart I). Conversely, the HOMO is mixed into the LUMO with the opposite phase. (This follows from the sign change of the denominator of the perturbation term upon reversing

---

(8) Program SURFACE II: Sampson, R. J. Kansas Geological Survey, University of Kansas: Lawrence, KS 66044.

(9) The phase with which the LUMO is mixed into the HOMO is given by the first-order perturbation theory term $\langle HOMO|F'|LUMO\rangle/(E_{HOMO} - E_{LUMO})$, where the first-named orbital is that to be perturbed by contamination from the second. In the current context, both the denominator and the numerator have negative values. On physical grounds, the numerator is negative because the perturbation operator F' bears a negative sign (owing to its origin in the decreased magnitude of the electron repulsion term in F), while the electron density function LUMO*HOMO has a positive sign when the LUMO and HOMO are like-phased at the perturbation site, as they are at B_g.

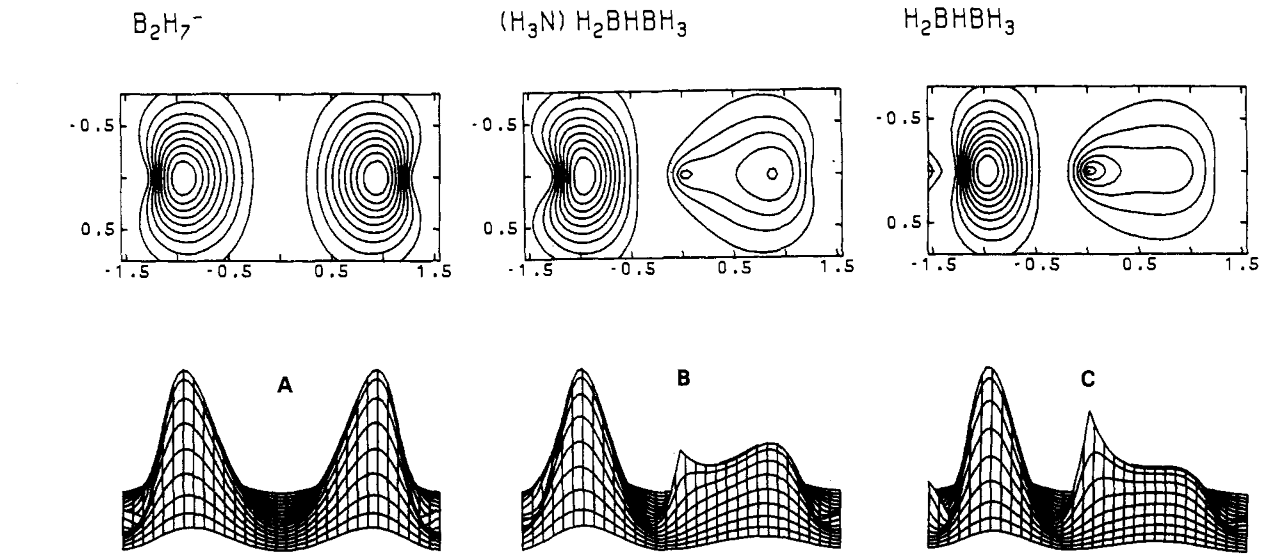

Figure 3. Density contour and surface maps: (A) $B_2H_7^-$; (B) $H_3NB_2H_6$; (C) "half-opened" B_2H_6 = $(H_2B)H(BH_3)$.

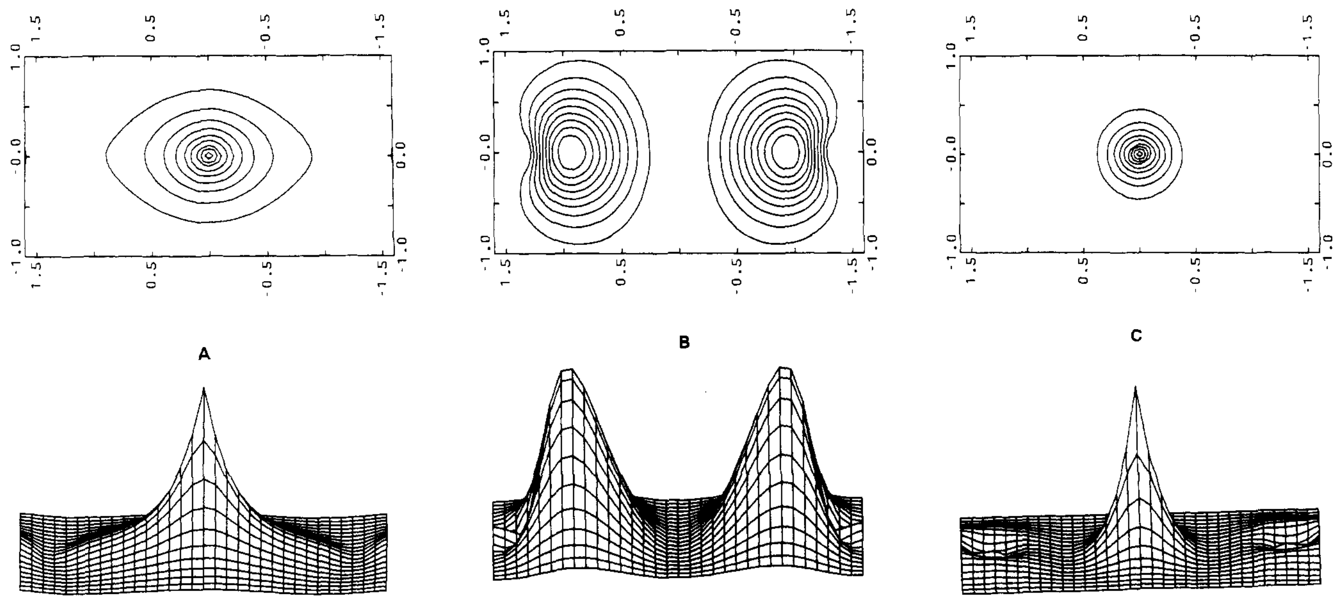

Figure 4. Bridge frontier orbital density contour and surface maps for $B_2H_7^-$: (A) HOMO; (B) LUMO; (C) NUMO.

the contaminating and contaminated orbitals). This leads to dipolarization of the LUMO (2′ in Chart I) in the opposite direction to that of the HOMO. Applied to the bridge orbital system, this so-called intuitive polarization produces a bridge LUMO dipolarized to the vicinal boron atom, in sharp disagreement with both experiment and the INDO results.

LUMO dipolarization counter to that just described arises when both the HOMO and LUMO are similarly dipolarized. This will be possible in a three-center orbital situation, which introduces a bridge NUMO (next unoccupied molecular orbital) lying above the LUMO. The NUMO will contaminate the LUMO so as to dipolarize the LUMO toward the perturbation site, B_g (2′ in Chart II). When the NUMO/LUMO energy gap is smaller than the LUMO/HOMO gap, NUMO contamination of the LUMO will dominate that of the HOMO, and the LUMO will be dipolarized toward, rather than away from, the perturbation site. Also of significance for the reactivity of **1**, the LUMO node will shift in this same direction from its originally symmetric position.

In $B_2H_7^-$ the NUMO, LUMO, and HOMO energies are (au) 0.542, 0.434, and −0.443. Thus, the LUMO/NUMO gap (0.108) is 8 times smaller than the LUMO/HOMO gap (0.877) for $B_2H_7^-$; by the arguments above, the LUMO becomes "counterintuitively" dipolarized toward B_g when the highly electron donating terminal ligand H^- is replaced by a less donating ligand, as was seen to be the case in Figure 2.

Chart II

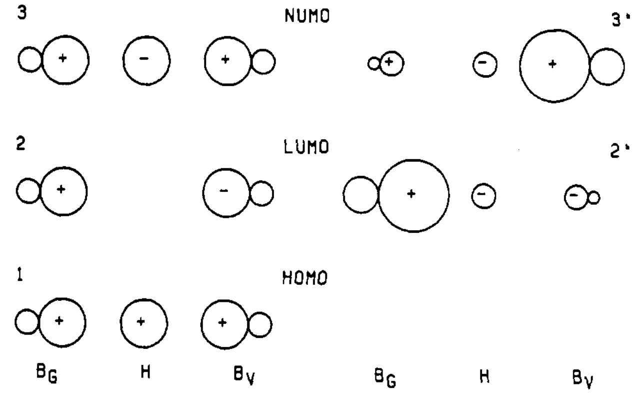

Dissociative Fragmentation of $(LH_2B)H(BH_3)$. The preceding discussion has focused on substrate orbital steering of an entering nucleophile as the basis for regiospecificity in the cleavage of **1**. It is also possible that a dissociative mechanism prevails. The following arguments again reveal that asymmetric cleavage is expected.

In contrast to the central roles of both the LUMO and HOMO in interchange reaction steps, only a single electron pair (that of

Scheme I

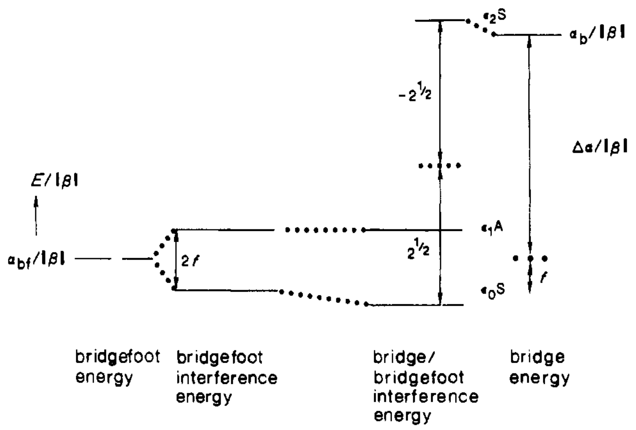

the HOMO) must be dealt with in a dissociative reaction step. During dissociative motion of the boron atoms of **1** the HOMO electron pair will distort owing to mixing of the LUMO into the HOMO. The phasing of the LUMO when it adds to the HOMO may, a priori, be positive or negative. Referring to LUMO 2′ of Chart II and HOMO 1′ of Chart I, notice that, regardless of the sign with which the LUMO is added to the HOMO, the nodal position of the LUMO is such that its mixing into the HOMO will produce cleavage of B_g–H rather than of B_v–H: the cleavage is necessarily unsymmetrical. The LUMO phasing will, however, determine onto which B atom the HOMO pair is directed: positive phasing of the LUMO will direct the HOMO electron pair onto B_g, producing the bizarre, high-energy products $LH_2B:^-$ and electron-deficient BH_4^+. In orbital correlation language, the HOMO evolves into a lone-pair orbital at B_g while the LUMO evolves into a BH_4^+ bonding orbital. Negative phasing of the LUMO directs the HOMO electron pair onto the bridging H and B_v atoms to give the more reasonable species LH_2B^+ and BH_4^- as products; in this instance, the HOMO evolves into a bonding orbital of the anion. Addition of L to LBH_2^+ consummates the reaction.

Effect of Bridge Orbital Electronegativity and Type. Given that hydrogen as a bridging unit is a rather special case, one wonders what can be said in general about bridging units in inorganic structures. Such structures are immensely important to describing inner-sphere electron-transfer reactions, bridged mixed-valence compounds, and bimetallic metalloorganic catalysts.

In bridge-cleavage reactions there is a dependence of substrate orbital steering on the relative NUMO/LUMO and LUMO/HOMO energy gaps. The latter are determined by the relative energies (electronegativities are the working analogues for many chemists) of the bridge unit orbital and the flanking orbitals with which it interferes. Also of potential significance is the symmetry of the bridge unit orbital. The question is "how does the direction of LUMO polarization depend on the energy/symmetry properties of the bridge unit atomic orbitals?"

To begin, we refer to the flanking atoms as bridgefeet and identify an atomic orbital, of energy α_{bf}, on each to interfere with the bridge unit atomic orbital of energy α_b. The two interference energies to consider are that of the bridge with a bridgefoot, β, and the longer range interference of the bridgefeet, β_{bf}. It will be convenient to normalize these energies to $|\beta|$: $\Delta\alpha/|\beta| = (\alpha_b - \alpha_{bf})/|\beta|$ and $f = -\beta_{bf}/|\beta| > 0$ (see Scheme I[10]). In this way the bridge/bridgefoot energy match and the long-range bridgefoot interaction can be related to the steering of the entering ligand.

Scheme II

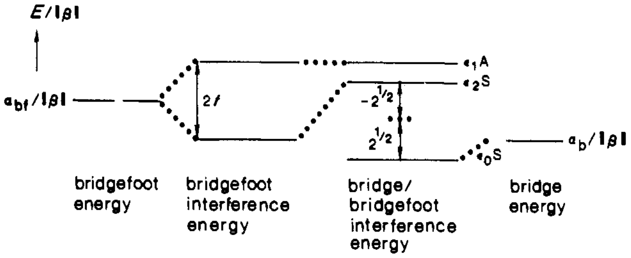

Normally, one expects to find the two-node bridge MO at higher energy than the one-node MO, leading to the customary (NUMO, LUMO, HOMO) sequence denoted SAS in Scheme I and found for $(H_3B)H(BH_3)^-$. In a general treatment it is prudent to recognize that there may be an inversion of the two- and one-node MO's, leading to the sequence ASS. This changes the spatial form of the LUMO and can alter the nature of the cleavage products. Scheme II illustrates the ASS ordering for the case $\alpha_b/|\beta| << \alpha_{bf}/|\beta|$.

The "inverted" sequence ASS will arise if the bridge orbital is sufficiently more stable than the bridgefoot orbital (lowering the two-node orbital) and/or f is sufficiently large (raising the one-node orbital). It is convenient to distinguish the cases of $\Delta\alpha/|\beta|$ greater and less than $-f$ as the "high" and "low" bridge cases, since $-f$ denotes the normalized energy shift of the symmetric, no-node bridgefoot orbital from α_{bf}; "high" and "low" therefore distinguish the situations with the bridge orbital above or below the no-node bridgefoot orbital with which it interferes (see the right side of Scheme I, where these quantities are marked).

	high bridge	low bridge
$\Delta\alpha/|\beta|$	$>-f$	$<-f$

The SAS and ASS orbital sequences have greatly different consequences for the polarization of the LUMO. Recognizing that A ↔ S mixing results in *di*polarization of the unperturbed MO's and that S ↔ S mixing results in *quadru*polarization, the possibilities for LUMO polarization by the NUMO and by the HOMO for the SAS and ASS sequences may be summarized as

	SAS	ASS
NUMO	SA, dipolar, gem	AS, dipolar, gem
HOMO	AS, dipolar, vic	SS, quadrupolar, to bridge

These four situations are defined by relations between $\Delta\alpha/|\beta|$ and f and are described graphically as in Figure 5A (the Appendix gives the details). Figure 5A has four regions identified by (a) the bridge orbital energy sequence, (b) the dominant contaminator of the LUMO, and (c) the resulting polarization of the LUMO.

Interpretation of Figure 5A is as follows. For either orbital sequence, A ↔ S mixing gives dipolarization of the A and S orbitals while S ↔ S mixing gives quadrupolarization of both S orbitals. It is to be expected that the long-range bridgefoot interference will be much less than the bridge/bridgefoot interference, so that the region $0 < f < 1$ is the one of practical concern.

Quadrupolarization of the LUMO arises for the ASS, HOMO region (the shaded area at the lower right), which requires f to be greater than 1.5 and so is unlikely to be observed. In the region $f < 1$, one expects geminal LUMO polarization for both SAS and ASS sequences, unless, under the SAS sequence, the bridge atomic orbital lies above the bridgefoot atomic orbital ($\Delta\alpha > 0$) and that gap is more than 3 times the magnitude of the long-range bridgefoot interference energy (the upper left shaded region). In practice, this is not a very great restriction when f is small, and it is quite possible that vicinal polarization can be observed in many inorganic bridged molecules $(L_{n-1}XM)E(ML_n)$ when M has orbitals more low-lying than E. Mechanistically this means that bridge cleavage can occur by nucleophilic attack at the less electronegative bridgefoot atom in an asymmetric bridge structure:

$$(L_{n-1}XM)E(ML_n) + N \rightarrow L_{n-1}XME + NML_n$$

---

(10) The one-node level in Scheme I is shown unshifted in energy. This is not found in practice, where, with $B_2H_7^-$ as an example, there is an upward shift in the energy of this molecular orbital. There are two origins of this effect: (1) increased electron–electron repulsions destabilize all one-electron molecular orbital energies upon the insertion of H^- into the H_3B---BH_3 unit; (2) more balanced boron valence s/p mixing is occasioned by the introduction of the bridge atom, and this enhances the long-range bridgefeet destructive interference.[3b] With $B_2H_7^-$ as an example, the boron s:p ratio in this molecular orbital changes from 19:81 to 40:60 ($sp^{4.2}$ to $sp^{1.5}$) upon insertion of the bridge H^- unit.

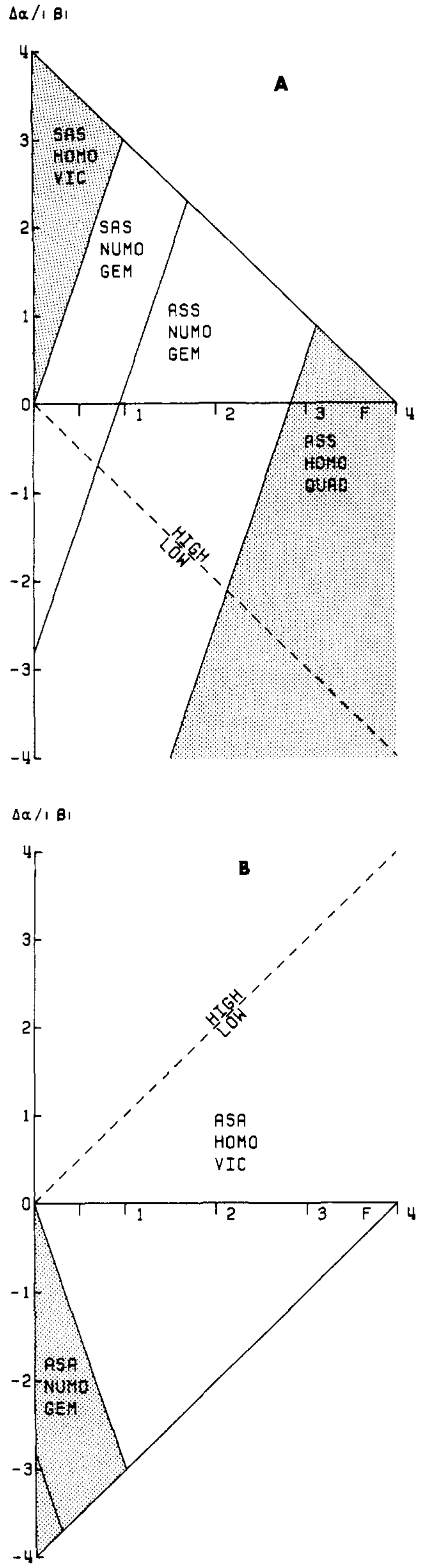

Figure 5. Graphical summary of the effects on LUMO polarization of the normalized bridge/bridgefoot orbital energy differential, $\Delta\alpha/|\beta|$, and bridgefoot interference energies, $f = -\beta_{bf}/|\beta|$: (A) s atomic bridge orbital; (B) bridging p atomic orbital.

where $L_{n-1}XM$ is more electronegative than ML_n. Otherwise, the cleavage will proceed as

$$(L_{n-1}XM)E(ML_n) + N \rightarrow L_{n-1}XMN + EML_n$$

through nucleophilic attack at the more electronegative bridgefoot, as found for **1**.

To this point, consideration has been given only to a symmetric bridge atomic orbital, appropriate to hydrogen as the bridging atom. Many bridged structures in inorganic chemistry feature a bridging halogen atom with an asymmetric p-type bridge orbital, and the question arises "how does the LUMO polarization depend on the symmetry of the bridge atomic orbital?" Figure 5B graphically describes the results detailed in the Appendix.

In Figure 5B, the quadrupolarization region that arises for the SAA, HOMO region falls far off-scale and is not shown. The vicinal HOMO polarization region dominates the $\Delta\alpha/|\beta|, f$ space. Geminal polarization (shaded area) arises only when $\Delta\alpha < 0$ and then only when the bridge/bridgefoot energy gap is more than 3 times the long-range bridgefoot interference; only a small portion of this SAA, LUMO, gem region satisfies the validity condition (the unlabeled, lower left triangular region).

Translated to observable chemistry, cleavage is expected at the less electronegative site, as in

$$(L_{n-1}XM)E(ML_n) + N \rightarrow L_{n-1}XME + NML_n$$

unless the M/E energy gap is more than three times the M/M long-range interference energy, in which case the cleavage will occur as

$$(L_{n-1}XM)E(ML_n) + N \rightarrow L_{n-1}XMN + EML_n$$

The Four-Orbital, Four-Electron Bridge. With both s and p bridge orbitals present, a composite of the individual S and A cases just presented arises. Strictly speaking, the three-center, three-orbital scheme of molecular orbital waves does not arise in these cases. A full examination of the four-orbital case reveals that when the bridge atom valence s, p atomic orbital energy gap is large only two stacking patterns are common for the NUMO, LUMO, HOMO sequence; these are readily distinguished by the symmetries of the bridge orbitals as [A(p*), S(s*), A(p)] and [A(p*), A(p), S(s*)] (the symbols in parentheses give the bridge atomic orbital type and its phasing with respect to the bridgefoot atom orbitals). These stacking sequences are precisely those of the three-center, three-orbital bridge p orbital case of Figure 5B. Accordingly, when the LUMO is polarized by the HOMO (A, S mixing) the LUMO is polarized vicinally and the cleavage reaction is

$$(L_{n-1}XM)E(ML_n) + N \rightarrow L_{n-1}XME + NML_n$$

When it is the NUMO that polarizes the LUMO, the cleavage is geminal (ASA sequence)

$$(L_{n-1}XM)E(ML_n) + N \rightarrow L_{n-1}XMN + EML_n$$

or quadrupolar (AAS sequence).

Summary

This study has revealed several important electronic steering features of bridge-cleavage reactions.

(1) A dipolarized bridge HOMO favors asymmetric bridge cleavage by a dissociative mechanism.

(2) Bridge molecular orbital sequences designated SAS and ASA lead to bridge LUMO dipolarization.

(3) Quadrupolarization of the LUMO is observable only for ASS and SAA orbital sequences and then only under strong, long-range bridgefoot interference or under great bridge/bridgefoot electronegativity difference.

(4) A dipolarized bridge LUMO will direct the entering nucleophile geminally or vicinally according to the sense of its polarization.

(5) Conversion of a hydrogen bridge structure to a halogen bridge structure tends to favor vicinal (symmetric) cleavage.

(6) The LUMO is polarized, and the steering biased, only when the bridgefoot groups are not identical.

(7) The LUMO node is displaced in the same direction as the LUMO, facilitating asymmetric or symmetric bridge cleavage.

(8) The *sense* of the LUMO polarization is *not* dictated *by the relative electronegativities of the two bridgefoot atoms* but *is dictated by the relative electronegativities* ($\Delta\alpha$) *of the bridge and bridgefoot groups* and *by the long-range bridgefoot interference*, which explicitly affect the relative HOMO and NUMO energy matches with the LUMO between them. The better the bridge/bridgefoot electronegativity balance, and the weaker the

long-range bridgefoot interference, the better the balance between the HOMO and the NUMO contaminations of LUMO, and therefore the less pronounced is the LUMO steering of the entering donor. This could become of paramount importance in sterically hindered bridge structures.

(9) The *relative electronegativities of the bridgefoot groups* determine the *magnitude* of the polarization, for it is this electronic asymmetry that drives the HOMO and NUMO mixings with the LUMO. Chemically, the greater the electron donation of the substituent ligand to the substituted bridgefoot atom, the less pronounced is the orbital steering. Whether the kinetically favored asymmetric product is actually observed depends on the temperature at which the product is isolated and on the steric congestion present during the nucleophile entry in the second interchange step.

Acknowledgment is made to the donors of the Petroleum Research Fund, asministered by the American Chemical Society, for support of this research.

Appendix

From the 2×2 secular determinant for the bridge/bridgefoot interference, the bridge orbital energies are

$$\text{S, two-node} \quad \epsilon_2 = (\alpha_b + \alpha_{bf} + \beta_{bf})/2 - 2^{1/2}\beta + \ldots$$

$$\text{A, one-node} \quad \epsilon_1 = \alpha_{bf} - \beta_{bf}$$

$$\text{S, no-node} \quad \epsilon_0 = (\alpha_b + \alpha_{bf} + \beta_{bf})/2 + 2^{1/2}\beta + \ldots$$

The higher order terms in ϵ_2 and ϵ_0 may be ignored if

$$-(4 + f) < \Delta\alpha/|\beta| < 4 - f$$

which becomes the validity condition for the following analysis.

The conditions for the SAS and ASS sequences are

	SAS	ASS
$\Delta\alpha/|\beta|$	$>-2(2^{1/2}) + 3f$	$<-2(2^{1/2}) + 3f$

For each of these two possibilities for bridge MO sequence, there are the two possibilities for LUMO polarization by either the HOMO or the NUMO. Quantitatively, these four possibilities are distinguished by the conditions on $\Delta\alpha/|\beta|$

	SAS	ASS
LUMO polarized by NUMO	$<3f$	$>-6(2^{1/2}) + 3f$
LUMO polarized by HOMO	$>3f$	$<-6(2^{1/2}) + 3f$

Construction of Figure 5A for an S bridge atomic orbital is as follows. $\Delta\alpha/|\beta|$, f space is divided into two regions corresponding to the SAS and ASS sequences by the line $\Delta\alpha/|\beta| = -2(2^{1/2}) + 3f$ in the center of Figure 5A. These two regions are subdivided by the NUMO, HOMO dominance conditions: $\Delta\alpha/|\beta| = 3f$ (SAS case) and $\Delta\alpha/|\beta| = -6(2^{1/2}) + 3f$ (ASS case). The validity condition $-(4 - f) < \Delta\alpha/|\beta| < 4 - f$ truncates the full space as shown by the upper solid diagonal line of negative slope (the lower limit is parallel to the upper but falls off scale in Figure 5A). The dashed line is included to distinguish the high- and low-bridge cases. The shaded areas denote LUMO polarization by the HOMO.

Replacement of the S bridge atom atomic orbital with an A orbital has the effects of changing S to A and A to S in the sequence codes (SAS, ASS → ASA, SAA) and of replacing f with $-f$ in all the conditions derived above for the S bridge orbital (because it is now the one-node A bridgefoot MO of normalized energy shift f that interferes with the bridge atom orbital). The change in sign of f provides a convenient relationship between the region divider lines in parts A and B of Figure 5: the dividers in Figure 5B are rotated from their positions in Figure 5A by an angle equal to twice that which its Figure 5A analogue makes with the f axis. Construction of Figure 5B is analogous to that of Figure 5A with the simple modification that the signs of the slopes of the space-dividing lines in Figure 5A are reversed.

Registry No. B_2H_6, 19287-45-7.

Contribution from the Department of Chemistry,
California State University, Los Angeles, California 90032

Reaction of the Small Closo Carboranes 1,6-$C_2B_4H_6$ and 2,4-$C_2B_5H_7$ with BX_3 (X = Halogen, Phenyl): A Method of Preparing "3"-Substituted 2,4-$C_2B_5H_7$ Derivatives and Preparation of 2-Br_2B-*closo*-1,6-$C_2B_4H_5$

Wonwoo Nam and Thomas Onak*

Received July 22, 1986

The reaction of *closo*-2,4-$C_2B_5H_7$ with BX_3 (X = Cl, Br, I, C_6H_5) at elevated temperatures (270 °C for BCl_3, 160 °C for BBr_3, 120 °C for BI_3, 160 °C for $B(C_6H_5)_3$) results in halogen, or phenyl, substitution primarily at the 3-position of the carborane (i.e. 3-X-*closo*-2,4-$C_2B_5H_6$). *closo*-2,4-$C_2B_5H_7$ also reacts with $(CH_3)_3CCl$ at 270 °C to give 3-Cl-*closo*-2,4-$C_2B_5H_6$. A closo carborane containing a trigonal boron σ-bonded to a cage carborane, 2-Br_2B-*closo*-1,6-$C_2B_4H_5$, is prepared from *closo*-1,6-$C_2B_4H_6$ and BBr_3 at 265 °C.

Introduction

Halogenations of *closo*-2,4-$C_2B_5H_7$ utilizing X_2 (X = Cl, Br, I) and Friedel–Crafts type catalysts have been found to result in the formation of the 5-substituted isomer 5-X-*closo*-2,4-$C_2B_5H_6$, followed by the formation of 5,6-X_2-*closo*-2,4-$C_2B_5H_5$ (X = Cl,[1-3] Br,[4,5] I[5]). Further chlorination[6] of 5,6-Cl_2-2,4-$C_2B_5H_5$ in the presence of $AlCl_3$ gives nearly equal amounts of 1,5,6-Cl_3-*closo*-2,4-$C_2B_5H_4$ and 3,5,6-Cl_3-*closo*-2,4-$C_2B_5H_4$. Chlorination of *closo*-2,4-$C_2B_5H_7$ in a light-initiated reaction[1] produces a mixture of 1-Cl-, 3-Cl-, and 5-Cl-2,4-$C_2B_5H_6$, but mostly the last isomer. Equilibrium amounts of 3-X-2,4-$C_2B_5H_6$ (X = Cl, Br, I) isomer are found from the thermal rearrangement of 5-X-$C_2B_5H_6$,[3,5,6] but the separation of the "3"-isomer from the other *B*-X-*closo*-2,4-$C_2B_5H_6$ isomers is often very tedious. In the present study, a new way of preparaing 3-X-*closo*-2,4-$C_2B_5H_6$ (X = Cl, Br, I, C_6H_5) is presented. In addition, 2-Br_2B-*closo*-1,6-$C_2B_4H_5$, a

---

(1) Warren, R.; Paquin, D.; Onak, T.; Dunks, G.; Spielman, J. R. *Inorg. Chem.* **1970**, *9*, 2285–2287.

(2) Spielman, J. R.; Warren, R. G.; Bergquist, D. A.; Allen, J. K.; Marynick, D.; Onak, T. *Synth. React. Inorg. Met.-Org. Chem.* **1975**, *5*, 347–356.

(3) Takimoto, C.; Siwapinyoyos, G.; Fuller, K.; Fung, A. P.; Liauw, L.; Jarvis, W.; Millhauser, G.; Onak, T. *Inorg. Chem.* **1980**, *19*, 107–110.

(4) Olsen, R. R.; Grimes, R. N. *J. Am. Chem. Soc.* **1970**, *92*, 5072–5075.

(5) Ng, B.; Onak, T.; Banuelos, T.; Gomez, F.; DiStefano, E. W. *Inorg. Chem.* **1985**, *24*, 4091–4096.

(6) Abdou, Z. J.; Soltis, M.; Oh, B.; Siwap, G.; Banuelos, T.; Nam, W.; Onak, T. *Inorg. Chem.* **1985**, *19*, 2363–2367.

0020-1669/87/1326-0048$01.50/0